Accessing Rydberg-dressed interactions using many-body Ramsey dynamics

Rick Mukherjee,[*] Thomas C. Killian, and Kaden R. A. Hazzard

Department of Physics and Astronomy, Rice University, Houston, Texas 77005, USA
and Rice Center for Quantum Materials, Rice University, Houston, Texas 77005, USA

We demonstrate that Ramsey spectroscopy can be used to observe Rydberg-dressed interactions in a many-body system well within experimentally measured lifetimes, in contrast to previous research, which either focused on interactions near Förster resonances or on few-atom systems. We build a spin-$\frac{1}{2}$ from one level that is Rydberg-dressed and another that is not. These levels may be hyperfine or long-lived electronic states. An Ising spin model governs the Ramsey dynamics, which we demonstrate can be used to characterize the Rydberg-dressed interactions. Furthermore, the dynamics can differ significantly from that observed in other spin systems. As one example, spin echo can *increase* the rate at which coherence decays. The results also apply to bare (undressed) Rydberg states as a special case, for which we quantitatively reproduce recent ultrafast experiments without fitting.

I. INTRODUCTION

Ultracold Rydberg atoms allow one to process quantum information [1–7], study interacting many-body systems [8–18], and engineer nonlinear quantum optics [19–31]. These applications stem from the enormous van der Waals interactions between Rydberg atoms excited to large principal quantum numbers $n \sim 50$–70. Since these interactions are proportional to n^{11}, they are enhanced by many orders of magnitude compared to ground-state atoms [32,33]. These interactions inhibit the simultaneous excitation of neighboring atoms to Rydberg states; this is known as the "blockade effect" [34–38]. Experiments have measured Rydberg interactions using Ramsey spectroscopy [39–41] and their dramatic consequences, such as the formation of Rydberg crystals [42,43], and suppressed excitation number fluctuations in the blockade region [44–46]. These experiments were focused on interactions between bare Rydberg atoms, through either van der Waals interactions or Förster resonances.

Dressed Rydberg atoms, in which a small amount of Rydberg state is superposed with the ground state, enlarge the possible range of many-body physics by allowing further control of the interaction potential. The strength, shape, and state lifetime can be controlled by choosing the amount of Rydberg character in the dressed superposition of ground and Rydberg states. (We note that alternative methods exist to tune strength and shape, for example, utilizing Förster resonances [47].) In particular, the reduced Rydberg character extends the dressed state's lifetime relative to the bare Rydberg state, since a dominant contribution to the lifetime is often the decay due to spontaneous emission from the Rydberg state [48–50]. Interactions between Rydberg-dressed atoms have been predicted to lead to interesting phases of matter [51–57] and exciton transport [58,59], stabilize three-dimensional solitons [60], enable phase imprinting of a Bose-Einstein condensate [61], and serve as a resource for quantum metrology and quantum information [62–64]. An exciting recent breakthrough is the measurement of Rydberg-dressed interactions between two atoms [65], but observing these interactions in a many-body system remains a major outstanding goal [66].

In this paper, we show how current experiments can observe and characterize dressed Rydberg interactions by using Ramsey spectroscopy, where one probes a spin-$\frac{1}{2}$ created from two long-lived atomic states, one of which is Rydberg dressed. This Ramsey protocol directly accesses a regime where superpositions are crucial and can give rise to nonclassical correlations. Although similar to the Ramsey protocol that has been fruitfully applied to other many-body atomic and molecular systems [67–76], we find that the Rydberg atoms behave in qualitatively different ways because of the shape of the potential and because the ground-Rydberg and ground-ground interactions are negligible compared to the Rydberg-Rydberg interactions. The unique character of the Rydberg-dressed interaction also manifests itself in the dependence of the dynamics on the atom density, the dressed state excitation fraction, the spin echo, and the Rydberg state. Just one example of this distinct behavior is that the contrast decay of the Ramsey fringe is *faster* with an echo than without in several regimes, including low density, large dissipation, and small excitation fraction of dressed states.

The proposed Ramsey protocol offers two advantages for observing and characterizing the Rydberg-dressed interactions. The first is that the dynamics occurs rapidly, on time scales set directly by the Rydberg-dressed interaction. In contrast, alternative schemes that rely on detecting the influence of the Rydberg-dressed interactions on the motion of the atoms can require much longer time scales associated with the atomic motion in the trap. A second fundamental advantage is that the dynamics admits—as we show—exact analytic solutions. This is extremely rare in an interacting many-body system and allows for rigorous comparisons between theory and experiment without uncontrolled approximations.

The rest of our paper is structured as follows. Section II discusses the physical setup of Rydberg dressing, forming a spin-$\frac{1}{2}$, and performing Ramsey spectroscopy. Section III presents the equations for the Ramsey fringe contrast as a function of time, and Sec. IV shows how the shape of this function characterizes the interaction between Rydberg-dressed atoms in a many-body gas. Section V demonstrates that correlations develop during the Ramsey dynamics on the same time scale that the contrast decays, considering the case of atoms in a lattice for simplicity and experimental relevance.
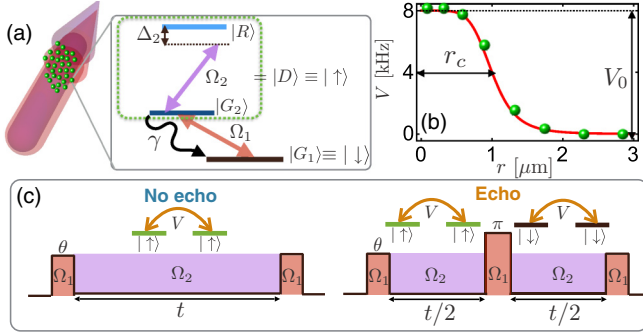
---

[*]rm47@rice.edu

FIG. 1. Probing dressed Rydberg interactions with Ramsey spectroscopy. (a) Atoms (green balls) are dressed and probed with two lasers. One laser (Ω_2, purple) weakly mixes the Rydberg state $|R\rangle$ into $|G_2\rangle$ to form the dressed state $|D\rangle$. This state is probed with strong pulses (Ω_1, red) that couple $|G_1\rangle$ and $|G_2\rangle$. (b) The Rydberg-dressed interaction for the $\Delta_2/C_6 < 0$ case considered herein has a height of V_0 and a soft-core radius, r_c. (c) Ramsey scheme: An initial Ω_1 pulse with area θ superposes $|\downarrow\rangle = |G_1\rangle$ and $|\uparrow\rangle = |D\rangle$ states. Dressed atoms interact between pulses. The final pulse allows one to measure the spin vector. One can apply a π echo pulse to eliminate single-particle imperfections. This also effectively "turns on" the interactions between atoms that were initially in the ground state for the second half of the dynamics.

Section VI applies our results to a special case that was recently realized in experiments, where one uses bare Rydberg states instead of Rydberg-dressed states. Good theory-experiment agreement in this special case provides a proof-of-principle for our proposed methods. Finally, Sec. VII concludes.

II. SETUP: RYDBERG DRESSING, INTERACTIONS, AND SPECTROSCOPY

We consider an atom with two long-lived levels, $|G_1\rangle$ and $|G_2\rangle$, as shown in Fig. 1(a). These could, for example, be two hyperfine states or the ground state and another sufficiently long-lived electronic state. A laser with Rabi frequency Ω_2 and detuning Δ_2 from resonance admixes a small fraction of the Rydberg state $|R\rangle$ to the $|G_2\rangle$ level. The eigenstate in the presence of this mixing is the Rydberg-dressed state $|D\rangle \approx |G_2\rangle + \epsilon|R\rangle$, with $\epsilon = (\Omega_2/2\Delta_2) \ll 1$. The Rydberg-dressed state can decay to $|G_1\rangle$ via spontaneous emission from either $|R\rangle$ or $|G_2\rangle$. The contribution to the decay rate of $|D\rangle$ from the Rydberg state is $\epsilon^2\Gamma_R$, where Γ_R is the spontaneous emission rate for the Rydberg state, while the contribution to $|D\rangle$'s decay from the $|G_2\rangle$ state is Γ_{G_2}, the spontaneous emission rate of $|G_2\rangle$. Which of these processes is important will depend on what states are chosen for $|G_2\rangle$ and $|R\rangle$. For example, if we use hyperfine ground states of Rb for $|G_1\rangle$ and $|G_2\rangle$, the spontaneous emission from $|G_2\rangle$ is negligible and the decay rate of $|D\rangle$ is $\epsilon^2\Gamma_R$.

The system we often employ for numerical examples is Sr with $|G_2\rangle$ chosen to be the $^3P_1$ state with a 21-μs lifetime, the same scheme employed in Ref. [63]. The $^3P_0$ clock state in Sr would be another interesting choice for $|G_2\rangle$, with a 159-s lifetime. In the case of Sr, the typical lifetimes for the Rydberg state ($n = 40$–70 s) is on the order of 5 μs [77,78] and we typically choose $\epsilon \sim 0.1$. The contribution to the

spontaneous emission of the dressed state from the Rydberg state is therefore $\epsilon^2\Gamma_R \approx 0.01 \times 1/(5\ \mu s) \approx 2\ ms^{-1}$. This is negligible compared to the $\gamma = 1/(21\ \mu s)$ decay rate of $^3P_1$, and we may take γ as the sole contribution to the spontaneous emission from the $|D\rangle$ state.

Our spin-$\frac{1}{2}$ system is then formed from $|\downarrow\rangle = |G_1\rangle$ and $|\uparrow\rangle = |D\rangle$. Here we assume that the positions of the atoms are fixed, which is an excellent approximation for ultracold systems over the time scales we consider. The interaction Hamiltonian for such a gas of atoms projected onto the spin-$\frac{1}{2}$ states is, up to an irrelevant constant [63],

$$\hat{H} = (1/2)\sum_{j\neq k}\left[(V_{jk}/4)\,\sigma_j^z\sigma_k^z + (V_{jk}/2)\,\sigma_k^z\right], \quad (1)$$

where $\sigma_k^z = (|\uparrow\rangle_k\langle\uparrow|_k - |\downarrow\rangle_k\langle\downarrow|_k)$, and we set $\hbar = 1$. The interaction between dressed atoms j and k with interatomic distance r_{jk} is $V_{jk} = V(r_{jk}) = V_0/[1 + (r_{jk}/r_c)^6]$, where $r_c = |C_6/2\Delta_2|^{1/6}$ is the soft-core radius and $V_0 = \epsilon^4(2\Delta_2)$ is the height of the dressed potential as shown in Fig. 1(b). C_6 is the van der Waals coefficient, which depends on the Rydberg state used. This Hamiltonian is nothing more than rewriting the Rydberg-dressed interactions Hamiltonian—in which D-state atoms interact, while G_1-D and G_1-G_1 interactions are negligible—in terms of spin-$\frac{1}{2}$ operators. This structure is unique to Rydberg atoms, and it is the reason that the coefficients of the Ising term and the single-particle term are linked through their dependence on the V_{jk}.

Figure 1(c) shows the Ramsey protocols studied here. The first strong, resonant pulse, $(\Omega_1/2)(|\downarrow\rangle_k\langle\uparrow|_k + \text{H.c.})$, rotates the spins by θ around the y axis. The wave function immediately after this pulse is

$$|\psi(t=0)\rangle = \bigotimes_k(\cos(\theta/2)|\downarrow\rangle_k + \sin(\theta/2)|\uparrow\rangle_k), \quad (2)$$

where θ is proportional to the pulse area. During the Ramsey dark time t (the time where $\Omega_1 = 0$) [79], the system evolves by Eq. (1), developing correlations. The pulse Ω_2 can either be applied just during the Ramsey dark period or left on during the entire experiment: As long as the Ω_1 pulses are chosen to be strong and short enough, the effects of the Ω_2 laser will be negligible during the short Ω_1 pulses. After the dark time t, a second pulse rotates the spin component $\sigma_k^{\alpha=x,y}$ into the z axis, where it can be measured as the population difference of $|\uparrow\rangle$ and $|\downarrow\rangle$. Here $\sigma_k^x = (|\downarrow\rangle_k\langle\uparrow|_k + \text{H.c.})$ and $\sigma_k^y = i(|\downarrow\rangle_k\langle\uparrow|_k - \text{H.c.})$. The incoherent emission from $|G_2\rangle$ is described in a master equation by including the jump operator σ^- with rate γ [see Fig. 1(c)]. It is convenient to measure and analyze the contrast of the Ramsey fringe [80],

$$C(t) = |\sigma^+(t)| = \sqrt{\langle\sigma^x(t)\rangle^2 + \langle\sigma^y(t)\rangle^2}, \quad (3)$$

and the phase, $\phi(t) = \arctan[\sigma^y(t)/\sigma^x(t)]$. We define $\sigma^\alpha = \sum_k\sigma_k^\alpha$. We study the dynamics both with and without a spin-echo pulse, illustrated in Fig. 1(b). A π spin-echo pulse around the y axis (i.e., in phase with the first pulse) leaves the spin-model interactions invariant while removing single-particle terms from the Hamiltonian Eq. (1), as well as any additional single-particle inhomogeneities in σ_i^z. The resulting dynamics are equivalent to evolution for time t *without* an echo but with an effective Hamiltonian, $\hat{H}_{\text{echo}} = (1/2)\sum_{j\neq k}(V_{jk}/4)\sigma_j^z\sigma_k^z$ as

shown in Appendix A. The spin echo has rather unusual effects in the system of Rydberg atoms, as it effectively *turns on* interactions between the $|\downarrow\rangle$ states, as illustrated in Fig. 1(c).

III. CALCULATING THE RAMSEY CONTRAST AND PHASE

The spin dynamics of Eq. (1) together with the nontrivial effects of the dissipation has been obtained by solving the corresponding master equation in Refs. [81,82] (generalizing Refs. [83–85]) to obtain

$$\langle \sigma^+(t) \rangle = \sin\theta e^{-2\gamma t} \sum_k \prod_{j \neq k} f(V_{jk}t), \qquad (4)$$

where

$$f(X) = e^{(i\beta X - \gamma t)/2}\{\cos[(X - i\gamma t)/2] \\ + [(\gamma t - iX\cos\theta)/2]\text{sinc}[(X - i\gamma t)/2]\}. \quad (5)$$

Here $\beta = 0$ is for the dynamics with a spin echo while $\beta = 1$ is for no-echo dynamics. The function $f(X)$ often simplifies; for example, $f(X) = \cos(X/2)$ for $\theta = \pi/2$, $\beta = 0$, and $\gamma = 0$.

Although Eq. (3) allows us to calculate the dynamics once we know the atom positions, it often is impossible to measure the positions of all of the atoms. However, in a large enough system, the dynamics is expected to "self-average": $C(t)$ for a single configuration in a large system is equal to its average over all configurations, and therefore it is independent of the specific configuration. We model the atoms to be independently distributed with a uniform density, ρ, for simplicity. The assumption is quantitatively justified for an initially weakly interacting, not-too-degenerate gas. Rather remarkably, we are able to analytically perform this disorder average in the thermodynamic limit: we find that Eq. (4) simplifies to evaluating a one-dimensional integral (see Appendix B),

$$\langle \sigma^+(t) \rangle = \exp\left(-\rho \int 4\pi r^2 dr \, [1 - f(V(r)t)]\right). \quad (6)$$

We note that Eqs. (4) and (6) neglect losses due to ionization or molecular resonances. One way to avoid resonances is to confine atoms in a lattice with appropriate lattice spacings [86,87]. Recently it has also been shown that for large numbers of atoms, losses to other dipole-allowed Rydberg states can be significant [88–90]. Another relevant decoherence is a dephasing of the $|G_2\rangle$ level at rate γ_d as could result from laser noise; this can be included simply by multiplying $\langle \sigma^+ \rangle$ by $e^{-\gamma_d t}$. Including these effects is beyond the scope of this paper, but often they should be relevant only on time scales beyond those of interest here.

IV. CHARACTERIZING RYDBERG-DRESSED INTERACTIONS USING RAMSEY

In the absence of dissipation, Eq. (6) implies that the dimensionless parameters, $N_R = 4\pi\rho r_c^3/3$ and $V_0 t$ encapsulate the dependence of the dynamics on the density ρ, the van der Waals coefficient C_6, and optical parameters (Ω_2, Δ_2). Thus, we present the contrast in Figs. 2 and 3 as the function $C(N_R, V_0 t)$, from which one can easily extract the dynamics for any experiment by using the appropriate N_R and V_0. To
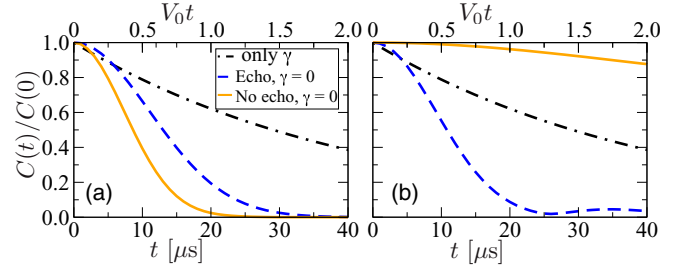

FIG. 2. Ramsey contrast versus time for a gas of ground-state Sr atoms with density $\rho = 10^{12}/\text{cm}^3$ dressed with 40-s triplet states with a dressing amplitude of $\epsilon = 0.1$. Panels (a) and (b) show $\theta = \pi/2$ and $\pi/20$, respectively. Individual curves are the dynamics in the absence of decoherence with and without spin echo ($\gamma = 0$ curves), compared to that of noninteracting atoms spontaneously emitting from only $|G_2\rangle$ with $\gamma = (21\ \mu\text{s})^{-1}$.

show typical scales, we also show the dynamics for typical Sr experimental parameters [91] with C_6 coefficients from Ref. [78]. These figures show $C(t)$ divided by its $t = 0$ value, so that, for example, the result is independent of the number of particles N in a homogeneous gas. Note, however, that the actual measured signal depends on N and θ.

Figure 2(a) demonstrates that the interaction-driven dynamics occurs on an experimentally favorable time scale, both with and without a spin echo. For example, in Sr the contrast dynamics for $\gamma = 0$ happens substantially faster than the spontaneous emission rate $\gamma = (21\ \mu\text{s})^{-1}$ of the $|G_2\rangle = |^3P_1\rangle$ state. Interesting behaviors emerge in the echo and nonecho dynamics. In a typical system, the dynamics without an echo pulse is faster than that with an echo pulse due to single-particle inhomogeneities. However, due to the unique structure of the Rydberg interactions, this naive intuition sometimes fails, as
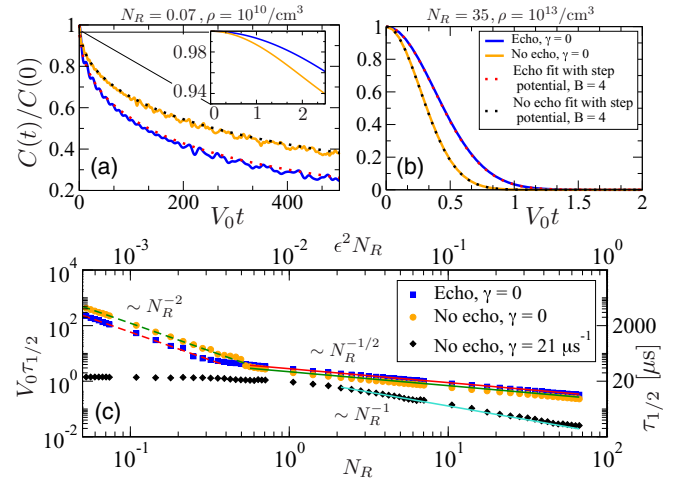

FIG. 3. (a,b) Contrast dynamics with $\theta = \pi/2$ and $\gamma = 0$ obtained from Eq. (7) takes a dramatically different shape in the $N_R \ll 1$ and $N_R \gg 1$ limits. Interestingly, for $N_R \ll 1$ the contrast dynamics is faster with echo than without, except at exceptionally short times (inset). The dashed lines are the analytic predictions of Eq. (6) for these limits. (c) Characteristic time scale for the dynamics as a function of N_R. The top x axis represents the average number of Rydberg excitations inside r_c.

seen in Fig. 2(b) for $\theta \ll 1$. In this case, the spin-echo pulse increases the effective interactions since it converts initially noninteracting $|G_1\rangle$ atoms into strongly interacting $|D\rangle$ states.

Figures 3(a) and 3(b) show that the contrast is sensitive to the shape of the potential, with striking differences in the low-density ($N_R \ll 1$) and high-density ($N_R \gg 1$) limits. These differences arise because for $N_R \ll 1$ the dynamics probes the $1/r^6$ interaction tail, while for $N_R \gg 1$ it probes the interaction potential inside the soft-core radius r_c. In these limits, the disorder-averaged contrast of Eq. (6) simplifies to

$$C(N_R, V_0 t) = \begin{cases} e^{-AN_R\sqrt{V_0 t}} & (N_R \ll 1), \\ e^{-BN_R[1-\cos^{\beta+1}(V_0 t)/2]} & (N_R \gg 1), \end{cases} \quad (7)$$

with $A = \sqrt{\pi}/2^{1+\beta/2}$ where $\beta = 0$ is for echo dynamics and $\beta = 1$ is for nonecho dynamics. For $N_R \ll 1$, this contrast is the exact solution of Eq. (6) and is nonanalytic at $t = 0$; thus it is beyond all orders of perturbation theory. For $N_R \gg 1$, Eq. (7) approximates $V(r) \approx V_0 H(r_c - r)$, where $H(x)$ is the Heaviside function. As shown in Fig. 3(b), this simple model reproduces the exact contrast up to an overall shift of the time scale: the naive $B = 1$ of the step function is replaced by $B = 4.0$ for the shown value of N_R.

The contrast dynamics depends on many system parameters, such as Ω_2, Δ_2, C_6, and ρ. One of the most important characteristics is the characteristic contrast decay time $\tau_{1/2}$, defined as $C(N_R, V_0\tau_{1/2}) = C(N_R, 0)/2$. Its dependence on the system parameters follows directly from Eq. (6) as

$$\tau_{1/2} \propto (N_R)^\alpha / V_0 \propto \Omega_2^{-4}\Delta_2^{3-\alpha/2}C_6^{\alpha/2}\rho^\alpha, \quad (8)$$

where $\alpha = -2$ for $N_R \ll 1$, while $\alpha = -1/2$ for $N_R \gg 1$. This scaling is confirmed in Fig. 3(c). Also note that Fig. 3(c)'s top axis shows $\epsilon^2 N_R$, which must be small in order for Eq. (1) to be valid.

Figure 3(c) also shows results for Sr including simultaneously interactions and dissipation with $\gamma = 1/(21 \, \mu s)$ (black diamonds). As in our previous results, this interaction-driven dynamics is faster than the spontaneous emission-only dynamics that occurs on the 21-μs time scale. However, in light of this, it is somewhat surprising that the dynamics in the presence of interactions and spontaneous emission simultaneously is much faster than for interactions alone. The reason is a back action of the emission events on the rest of the spins through the interaction: Each emission event affects a single spin, which through interactions causes a number of neighboring spins, $\sim N_R$, to precess significantly, thereby greatly amplifying the contrast dynamics and correlation growth beyond that caused by either interactions alone or spontaneous emission alone. This is analogous to the feedback effect explained in Ref. [81].

V. CORRELATIONS ARISING FROM RYDBERG-DRESSED INTERACTIONS IN A LATTICE

In this section we show that making more detailed measurements—in particular with spatial resolution—after the final Ramsey pulse further extends our ability to observe and characterize the Rydberg-dressed interaction. So far our calculations have been for a gas where both the excitation and the measurement are done collectively on the whole
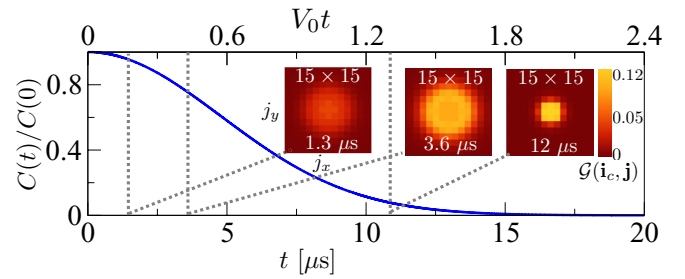

FIG. 4. Contrast and correlation dynamics in 15×15 square lattice with one particle per site. Dressing parameters are the same as those in Fig. 2. The lattice spacing is $a = 0.5 \, \mu$m and $r_c \approx 2a$. In the insets, we show the connected correlation function for the center atom located at $\mathbf{i}_c$ and the surrounding atoms using $\mathcal{G}(\mathbf{i},\mathbf{j})$ as defined in the text.

system; this is the typical and most straightforward case in current experiments. However, it is also possible to spatially resolve $\langle \sigma_i^x \rangle$ [92–94]. The extreme limit of this capability is the single-atom resolution that has recently been achieved in microscope experiments [42,43] for atoms in lattices. The images in these experiments reveal not only $\langle \sigma_i^x \rangle$ but also correlations such as $\langle \sigma_i^x \sigma_j^x \rangle$.

Motivated by these ongoing experiments, we study the Ramsey dynamics with a spin echo on a two-dimensional square lattice with exactly one particle per site. For simplicity we neglect spontaneous emission. Figure 4 shows the $C(t)$ and snapshots of the connected correlation [81,82] $\mathcal{G}(\mathbf{i},\mathbf{j}) = \langle \sigma_{\mathbf{i}}^x \sigma_{\mathbf{j}}^x \rangle - \langle \sigma_{\mathbf{i}}^x \rangle \langle \sigma_{\mathbf{j}}^x \rangle$, where $\mathbf{i}$ and $\mathbf{j}$ are two-dimensional vectors which define the lattice sites. We observe that the shape and time scale of the contrast dynamics is similar to the $N_R \gg 1$ limit found in the gas. The spatial structure of the Rydberg-dressed interactions is manifested in the spatial correlations, allowing rather direct characterization of the interactions.

Furthermore, Fig. 4 demonstrates that the decay of the contrast is associated with a growth of strong spin correlations within the radius r_c. Our calculations show this quite generally as long as decoherence is not too large. In fact, this link can be made even more general and rigorous without even relying on the specific Hamiltonian time evolution of Eq. (1). The contrast of a single spin i, $C_i = |\langle \sigma_i^+ \rangle|$, is identical for all uncorrelated (product) states with a given $\langle \sigma_i^z \rangle$. Therefore any decay of this single-spin contrast C_i must occur due to the growth of correlations. Of course, the collective contrast $C = |\sum_i \langle \sigma_i^+ \rangle|$ that we have focused on can decay due to relative precessions of different spins without the single-spin contrast C_i decaying; however, in the presence of an echo, such effects are expected to be absent. Thus, in the quite general situation of spin-echo dynamics in a closed system, we expect collective contrast decay to be associated with the growth of correlations.

VI. CHARACTERIZING BARE RYDBERG INTERACTIONS USING ULTRAFAST LASERS

We now consider a special case of our results that has in fact already been experimentally and theoretically studied in the literature, in which one utilizes bare Rydberg rather than Rydberg-dressed states [95]. In addition to exemplifying the generality of our calculations, this demonstrates a
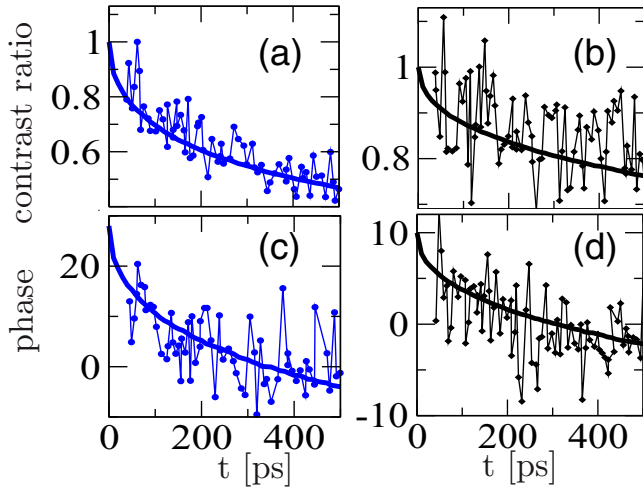
FIG. 5. Calculated contrast decay and phase shift for bare Rydberg atoms, which agrees with experimental measurements (taken from Ref. [95]). Left and right columns are for $f = 3.1\%$ and $f = 1.2\%$ of particles excited to the Rydberg state, i.e., $f = 1 - \cos\theta$, respectively. (a,b) Ratio of the contrast at $\rho = 1.3 \times 10^{12}$ cm^{-3} to the contrast at 4×10^{10} cm^{-3}. (c,d) Corresponding Ramsey phase, shifted at $t = 0$ as in the analysis in Ref. [95].

proof-of-principle of the ideas contained herein. For this case, V_{jk} is a pure van der Waals potential, $V(r_{jk}) = C_6/r_{jk}^6$. We show that the experimental data and much of the prior theoretical modeling can be reproduced as a special case of our results.

Typically, due to strong blockade effects, it is hard to excite atoms to superpositions of ground and bare Rydberg states at a sufficiently large density. However, by using strong, ultrafast lasers, Ref. [95] has overcome this difficulty and couples Rb atoms from their ground state $|G\rangle$ to the bare $42D_{5/2}$ Rydberg state $|R\rangle$.

Figure 5 shows our calculations of the contrast and phase for this experiment, which did not apply a spin-echo pulse. We used $|C_6| = 9.8$ GHz-μm^6, taken from Ref. [96], and densities ρ taken from Ref. [95] with values indicated in the caption to Fig. 5. Our results quantitatively agree with experiment without any fitting. We emphasize that the theoretical results of Ref. [95] agree equally well with the data, and when our theory is applied to the same potential it reduces to theirs. Our main point here is to demonstrate that this bare Rydberg dynamics emerges as a special case of our results.

The agreement between theory and experiment confirms that the effects of Zeeman degeneracies [97] can be neglected, possibly because at the low fraction of Rydberg excitation studied the excitations are far enough separated that short-range resonances are negligible. The agreement provides a compelling proof of principle for Ramsey spectroscopy as a method in future ultracold Rydberg-dressed experiments.

VII. CONCLUSIONS

We have shown that the dynamics of the Ramsey fringe contrast happens on experimentally favorable time scales and allows one to access and characterize Rydberg-dressed

interactions in a many-body system. Quite remarkably for a many-body interacting system, we are able to provide exact analytic solutions for the contrast dynamics, despite the strongly correlated dynamics. (To emphasize the strong correlations, note that for $\theta = \pi/2$, the dynamics is completely beyond mean-field theory, which predicts a time-independent spin-echo contrast.)

The ability to solve the dynamics exactly contrasts with many other types of dynamics and spectroscopy, for which approximations must inevitably be made. For example, if we were to consider Rabi spectroscopy rather than Ramsey spectroscopy, no general procedure to solve the dynamics—even numerically—would be available; similarly, no techniques exist to efficiently calculate the Ramsey contrast dynamics of Rydberg atoms near a Förster resonance. In contrast to our Ramsey dynamics, calculating the dynamics in these other situations inevitably involves approximations. For example, to model dynamics near Förster resonances, Refs. [41,98] employed a model of the many-body dynamics as two-particle dynamics averaged over the expected nearest-neighbor inter-particle separation in a homogeneous gas (the Chandrasekhar distribution). While this is a useful and potentially accurate approximation in some circumstances, it has limits to its applicability. For example, at large N_R in our system, it would predict the dynamics decays at a rate of V_0 rather than $\sqrt{N_R} V_0$, a large error for $N_R \gg 1$.

The exact analytic solutions provided for the Ramsey contrast dynamics allow for systematic and rigorous comparison between experiment and theory, without uncertainties associated with approximate treatments. Such comparisons are extremely beneficial for diagnosing experimental complications. Discrepancies between theory and experiment cannot be blamed on approximations, but instead directly imply that an important aspect of the experiment has been omitted from the theory.

We showed, as a first step and proof of principle, that our theory quantitatively agrees with recent ultrafast measurements of bare Rydberg atoms, a remarkable demonstration of the universality of the dynamics over 6 orders of magnitude, from μs to ps. We revealed that the contrast dynamics is sensitive to the shape of the interaction potential, as well as to the density, the principal quantum number, and the dressing laser properties.

Striking dynamics emerges for $N_R \ll 1$: The contrast displays a nonperturbative short time nonanalyticity, $e^{-\sqrt{t/\tau_0}}$, due to the $1/r^6$ character of Rydberg interactions. Further interesting dynamical phenomena result from the unique nature of Rydberg interactions. For example, the spin-echo pulse enhances the rate of contrast dynamics for small excitation fraction θ or low densities.

Although previous experiments on coherent excitation of Rydberg atoms in many-body systems have demonstrated strong correlations, they have not established their *nonclassicality*. Although we do not show the nonseparability of the correlations, Ramsey spectroscopy directly creates and probes the superpositions necessary for quantum correlations. Such quantum correlations are expected to occur, despite the fact that Eq. (1) is "classical." Although in equilibrium the fact that the Hamiltonian consists of commuting variables does imply that correlations are classical (in the sense that entanglement is

absent), this is not true out of equilibrium: extremely entangled states can be and generically are generated dynamically by such Hamiltonians.

In the future, performing similar Ramsey experiments but with local pulses applied to read out various spin components would allow measurement of the quantumness in the correlations and would pave the way for studying interesting many-body nonequilibrium spin physics. Recently, Ref. [99] has used Ramsey spectroscopy to experimentally observe Rydberg-dressed interactions of atoms in an optical lattice using a quantum gas microscope with local readout capabilities, suggesting that measurement of genuine nonclassical correlations may be within reach. Another interesting direction is to simply add a transverse field. This prevents exact solution and the resulting rich many-body dynamics will be an interesting test bed for theoretical methods [100–103].

APPENDIX A: EFFECTIVE HAMILTONIAN FOR RAMSEY DYNAMICS WITH AN ECHO

In the nonecho dynamics protocol, the time-evolution operator for the Ramsey dark period is given by $U_{\text{nonecho}} = e^{-i\hat{H}t}$, where $\hat{H}$ is given by Eq. (1). For the spin-echo dynamics, the time-evolution operator is given by $U_{\text{echo}} = e^{-i\hat{H}t/2}R_\pi e^{-i\hat{H}t/2}$, where R_π is the π-pulse evolution. The combined effect of $R_\pi e^{-i\hat{H}t/2}$ is that the system evolves under a unitary transformation given by $e^{-i\hat{H}_R t/2}$, where $\hat{H}_R$ is same as $\hat{H}$ but with $\sigma_j^z \to -\sigma_j^z$:

$$\hat{H}_R = \frac{1}{2}\sum_{j\neq k}\left[(V_{jk}/4)\,\sigma_j^z\sigma_k^z - (V_{jk}/2)\,\sigma_k^z\right], \tag{A1}$$

so $U_{\text{echo}} = e^{-i\hat{H}t/2}e^{-i\hat{H}_R t/2}$. Since $\hat{H}$ and $\hat{H}_R$ commute, the resulting time-evolution operator is $U_{\text{echo}} = e^{-i\hat{H}_{\text{echo}}t}$, where $\hat{H}_{\text{echo}} = (\hat{H} + \hat{H}_R)/2$. Physically this implies that interactions between atoms initially in $|G_1\rangle$ states start interacting in the

second half of the spin-echo dynamics. Additional contributions arising from interactions with atoms in $|G_1\rangle$ and $|D\rangle$ states are negligible.

APPENDIX B: ANALYTIC EXPRESSION OF CONTRAST FOR A UNIFORMLY DISTRIBUTED GAS OF ATOMS

For the derivation of Eq. (6), consider a uniformly distributed gas of N atoms with positions labeled by j and k. Since the particles are independent, the probability distribution in space factors as $P(\mathbf{r}_1, \mathbf{r}_2, \ldots, \mathbf{r}_N) = P(\mathbf{r}_1)P(\mathbf{r}_1)\cdots P(\mathbf{r}_N)$. For a uniform distribution, we have $P(\mathbf{r}_j) = \rho/N$, where ρ is the uniform density of the gas. Thus averaging Eq. (4) in the main text, we have

$$\langle\sigma_k^+(t)\rangle = \int d\mathbf{r}_1 \cdots d\mathbf{r}_{N-1}\left(\frac{\rho}{N-1}\right)^{N-1}\prod_{j\neq k} f(V(r_{jk})t)$$

$$= \left(\frac{\rho}{N-1}\right)^{N-1}\prod_{j\neq k}\left[\int d\mathbf{r}_j\, f(V(r_{jk})t)\right]$$

$$= \left[\left(\frac{\rho}{N-1}\right)\int d\mathbf{r}_j\, f(V(r_{jk})t)\right]^{N-1}. \tag{B1}$$

Although the remaining single integral diverges with the system volume this divergence is canceled by the $1/(N-1)$ factor. To evaluate the expression in Eq. (B1) it is convenient to define the finite integral

$$\mathcal{I} = \rho\int 4\pi r^2 dr[1 - f(V(r)t)], \tag{B2}$$

in terms of which Eq. (B1) simplifies to

$$\langle\sigma_k^+(t)\rangle = \left[1 - \frac{\mathcal{I}}{N}\right]^{N-1}. \tag{B3}$$

In the thermodynamic limit where $N \to \infty$, the above expression is

$$\langle\sigma^+(t)\rangle = \exp\left(-\rho\int 4\pi r^2 dr[1 - f(V(r)t)]\right), \tag{B4}$$

which is Eq. (6) in the main text. We emphasize that no approximation or redefinition is made in our calculation to render it finite: the diverging integral in Eq. (B1) simply cancels out in the final expression. Note that this simplified expression depends on the function f, which in turn depends on the exact dynamics (echo, nonecho, tipping angle, dissipation). Our results coincide with those of Ref. [95] in the special cases calculated there.

---

[1] D. Jaksch, J. I. Cirac, P. Zoller, S. L. Rolston, R. Cote, and M. D. Lukin, Phys. Rev. Lett. **85**, 2208 (2000).

[2] M. D. Lukin, M. Fleischhauer, R. Cote, L. M. Duan, D. Jaksch, J. I. Cirac, and P. Zoller, Phys. Rev. Lett. **87**, 037901 (2001).

[3] A. Gaëten *et al.*, Nat. Phys. **5**, 115 (2009).

[4] E. Urban *et al.*, Nat. Phys. **5**, 110 (2009).

[5] L. Isenhower, E. Urban, X. L. Zhang, A. T. Gill, T. Henage, T. A. Johnson, T. G. Walker, and M. Saffman, Phys. Rev. Lett. **104**, 010503 (2010).

[6] T. Wilk, A. Gaetan, C. Evellin, J. Wolters, Y. Miroshnychenko, P. Grangier, and A. Browaeys, Phys. Rev. Lett. **104**, 010502 (2010).

[7] M. Saffman, T. G. Walker, and K. Mølmer, Rev. Mod. Phys. **82**, 2313 (2010).

[8] H. Weimer, R. Löw, T. Pfau, and H. P. Büchler, Phys. Rev. Lett. **101**, 250601 (2008).

[9] B. Olmos, R. Gonzàlez-Fèrez, and I. Lesanovsky, Phys. Rev. Lett. **103**, 185302 (2009).

[10] I. Lesanovsky, B. Olmos, and J. P. Garrahan, Phys. Rev. Lett. **105**, 100603 (2010).

[11] I. Lesanovsky, Phys. Rev. Lett. **106**, 025301 (2011).

[12] T. Pohl, E. Demler, and M. D. Lukin, Phys. Rev. Lett. **104**, 043002 (2010).

[13] M. Viteau, M. G. Bason, J. Radogostowicz, N. Malossi, D. Ciampini, O. Morsch, and E. Arimondo, Phys. Rev. Lett. **107**, 060402 (2011).

[14] C. S. Hofmann, G. Gunter, H. Schempp, M. Robert-de-Saint-Vincent, M. Garttner, J. Evers, S. Whitlock, and M. Weidemuller, Phys. Rev. Lett. **110**, 203601 (2013).

[15] C. Carr, R. Ritter, C. G. Wade, C. S. Adams, and K. J. Weatherill, Phys. Rev. Lett. **111**, 113901 (2013).

[16] I. Lesanovsky and J. P. Garrahan, Phys. Rev. A **90**, 011603(R) (2014).

[17] A. Dauphin, M. Müller, and M. A. Martin-Delgado, Phys. Rev. A **86**, 053618 (2012).

[18] A. Dauphin, M. Müller, and M. A. Martin-Delgado, Phys. Rev. A **93**, 043611 (2016).

[19] Y. O. Dudin and A. Kuzmich, Science **336**, 887 (2012).

[20] Y. O. Dudin *et al.*, Nat. Phys. **8**, 790 (2012).

[21] K. J. Weatherill *et al.*, J. Phys. B **41**, 201002 (2008).

[22] A. K. Mohapatra, T. R. Jackson, and C. S. Adams, Phys. Rev. Lett. **98**, 113003 (2007).

[23] J. D. Pritchard, D. Maxwell, A. Gauguet, K. J. Weatherill, M. P. A. Jones, and C. S. Adams, Phys. Rev. Lett. **105**, 193603 (2010).

[24] D. Petrosyan, J. Otterbach, and M. Fleischhauer, Phys. Rev. Lett. **107**, 213601 (2011).

[25] V. Parigi, E. Bimbard, J. Stanojevic, A. J. Hilliard, F. Nogrette, R. Tualle-Brouri, A. Ourjoumtsev, and P. Grangier, Phys. Rev. Lett. **109**, 233602 (2012).

[26] T. Peyronel *et al.*, Nature (London) **488**, 57 (2012).

[27] A. V. Gorshkov, J. Otterbach, M. Fleischhauer, T. Pohl, and M. D. Lukin, Phys. Rev. Lett. **107**, 133602 (2011).

[28] O. Firstenberg *et al.*, Nature (London) **502**, 71 (2013).

[29] D. Chang, V. Vuletić, and M. D. Lukin, Nat. Photonics **8**, 685 (2014).

[30] D. Maxwell, D. J. Szwer, D. Paredes-Barato, H. Busche, J. D. Pritchard, A. Gauguet, K. J. Weatherill, M. P. A. Jones, and C. S. Adams, Phys. Rev. Lett. **110**, 103001 (2013).

[31] L. Li, Y. O. Dudin, and A. Kuzmich, Nature (London) **498**, 466 (2013).

[32] P. Bohlouli-Zanjani, J. A. Petrus, and J. D. D. Martin, Phys. Rev. Lett. **98**, 203005 (2007).

[33] L. Beguin, A. Vernier, R. Chicireanu, T. Lahaye, and A. Browaeys, Phys. Rev. Lett. **110**, 263201 (2013).

[34] D. Tong, S. M. Farooqi, J. Stanojevic, S. Krishnan, Y. P. Zhang, R. Cote, E. E. Eyler, and P. L. Gould, Phys. Rev. Lett. **93**, 063001 (2004).

[35] K. Singer, M. Reetz-Lamour, T. Amthor, L. G. Marcassa, and M. Weidemuller, Phys. Rev. Lett. **93**, 163001 (2004).

[36] T. Vogt, M. Viteau, J. Zhao, A. Chotia, D. Comparat, and P. Pillet, Phys. Rev. Lett. **97**, 083003 (2006).

[37] R. Heidemann, U. Raitzsch, V. Bendkowsky, B. Butscher, R. Low, L. Santos, and T. Pfau, Phys. Rev. Lett. **99**, 163601 (2007).

[38] D. Comparat and P. Pillet, J. Opt. Soc. Am. B **27**, 208 (2010).

[39] W. R. Anderson, M. P. Robinson, J. D. D. Martin, and T. F. Gallagher, Phys. Rev. A **65**, 063404 (2002).

[40] J. Nipper, J. B. Balewski, A. T. Krupp, B. Butscher, R. Low, and T. Pfau, Phys. Rev. Lett. **108**, 113001 (2012).

[41] J. Nipper, J. B. Balewski, A. T. Krupp, S. Hofferberth, R. Low, and T. Pfau, Phys. Rev. X **2**, 031011 (2012).

[42] P. Schauss *et al.*, Nature (London) **491**, 87 (2012).

[43] P. Schauss *et al.*, Science **347**, 6229 (2015).

[44] M. Viteau, P. Huillery, M. G. Bason, N. Malossi, D. Ciampini, O. Morsch, E. Arimondo, D. Comparat, and P. Pillet, Phys. Rev. Lett. **109**, 053002 (2012).

[45] N. Malossi, M. M. Valado, S. Scotto, P. Huillery, P. Pillet, D. Ciampini, E. Arimondo, and O. Morsch, Phys. Rev. Lett. **113**, 023006 (2014).

[46] T. Cubel Liebisch, A. Reinhard, P. R. Berman, and G. Raithel, Phys. Rev. Lett. **95**, 253002 (2005); **98**, 109903 (2007).

[47] D. B. Tretyakov, V. M. Entin, E. A. Yakshina, I. I. Beterov, C. Andreeva, and I. I. Ryabtsev, Phys. Rev. A **90**, 041403(R) (2014).

[48] J. Honer, H. Weimer, T. Pfau, and H. P. Buchler, Phys. Rev. Lett. **105**, 160404 (2010).

[49] J. E. Johnson and S. L. Rolston, Phys. Rev. A **82**, 033412 (2010).

[50] J. B. Balewski *et al.*, New J. Phys. **16**, 063012 (2014).

[51] N. Henkel, R. Nath, and T. Pohl, Phys. Rev. Lett. **104**, 195302 (2010).

[52] F. Cinti, P. Jain, M. Boninsegni, A. Micheli, P. Zoller, and G. Pupillo, Phys. Rev. Lett. **105**, 135301 (2010).

[53] G. Pupillo, A. Micheli, M. Boninsegni, I. Lesanovsky, and P. Zoller, Phys. Rev. Lett. **104**, 223002 (2010).

[54] M. Mattioli, M. Dalmonte, W. Lechner, and G. Pupillo, Phys. Rev. Lett. **111**, 165302 (2013).

[55] M. Dalmonte, W. Lechner, Z. Cai, M. Mattioli, A. M. Lauchli, and G. Pupillo, Phys. Rev. B **92**, 045106 (2015).

[56] R. M. W. van Bijnen and T. Pohl, Phys. Rev. Lett. **114**, 243002 (2015).

[57] A. W. Glaetzle, M. Dalmonte, R. Nath, C. Gross, I. Bloch, and P. Zoller, Phys. Rev. Lett. **114**, 173002 (2015).

[58] S. Wuester *et al.*, New J. Phys. **13**, 073044 (2011).

[59] H. Schempp, G. Gunter, S. Wuster, M. Weidemuller, and S. Whitlock, Phys. Rev. Lett. **115**, 093002 (2015).

[60] F. Maucher, N. Henkel, M. Saffman, W. Krolikowski, S. Skupin, and T. Pohl, Phys. Rev. Lett. **106**, 170401 (2011).

[61] R. Mukherjee, C. Ates, W. Li, and S. Wuster, Phys. Rev. Lett. **115**, 040401 (2015).

[62] I. Bouchoule and K. Molmer, Phys. Rev. A **65**, 041803(R) (2002).

[63] L. I. R. Gil, R. Mukherjee, E. M. Bridge, M. P. A. Jones, and T. Pohl, Phys. Rev. Lett. **112**, 103601 (2014).

[64] T. Keating, K. Goyal, Y. Y. Jau, G. W. Biedermann, A. J. Landahl, and I. H. Deutsch, Phys. Rev. A **87**, 052314 (2013).

[65] Y. Y. Jau *et al.*, Nat. Phys. **12**, 71 (2016).

[66] W. Li, L. Hamadeh, and I. Lesanovsky, Phys. Rev. A **85**, 053615 (2012).

[67] B. Yan *et al.*, Nature (London) **501**, 521 (2013).

[68] X. Zhang *et al.*, Science **345**, 1467 (2014).

[69] A. M. Rey *et al.*, Ann. Phys. **340**, 311 (2014).

[70] K. R. A. Hazzard, S. R. Manmana, M. Foss-Feig, and A. M. Rey, Phys. Rev. Lett. **110**, 075301 (2013).

[71] K. R. A. Hazzard, B. Gadway, M. Foss-Feig, B. Yan, S. A. Moses, J. P. Covey, N. Y. Yao, M. D. Lukin, J. Ye, D. S. Jin, and A. M. Rey, Phys. Rev. Lett. **113**, 195302 (2014).

[72] M. Wall, K. R. A. Hazzard, and A. M. Rey, Chapter in *From Atomic to Mesoscale: The Role of Quantum Coherence in Systems of Various Complexities*, edited by S. Malinovskaya and I. Novikova (World Scientific, Singapore, 2015).

[73] M. Knap, A. Kantian, T. Giamarchi, I. Bloch, M. D. Lukin, and E. Demler, Phys. Rev. Lett. **111**, 147205 (2013).

[74] S. Trotzky *et al.*, Phys. Rev. Lett. **114**, 015301 (2015).

[75] M. Koschorreck *et al.*, Nat. Phys. **9**, 405 (2013).

[76] K. R. A. Hazzard, M. van den Worm, M. Foss-Feig, S. R. Manmana, E. G. Dalla Torre, T. Pfau, M. Kastner, and A. M. Rey, Phys. Rev. A **90**, 063622 (2014).

[77] C. J. Dai and X. A. Zhao, J. Quant. Spectrosc. Radiat. Transfer **54**, 1019 (1995).

[78] C. L. Vaillant, M. P. A. Jones, and R. M. Potvliege, J. Phys. B **47**, 155001 (2014).

[79] We choose to describe the dynamics in terms of parameters Ω_2 and t rather than this laser's pulse area, $\Omega_2 t$. Because Ω_2 is a dressing laser rather than a term driving spin rotations of the spin-$\frac{1}{2}$, the $\Omega_2 t$ pulse area does not arise as a natural parameter to characterize the dynamics; this dimensionless combination does not naturally enter any of the expressions for the dynamics.

[80] This is the conventional definition of the Ramsey contrast, as defined in, e.g., P. Meystre and M. Sargent, in *Elements of Quantum Optics*, 4th ed. (Springer, New York, 2007), Eq. (1.86).

[81] M. Foss-Feig *et al.*, New J. Phys. **15**, 113008 (2013).

[82] M. Foss-Feig, K. R. A. Hazzard, J. J. Bollinger, and A. M. Rey, Phys. Rev. A **87**, 042101 (2013).

[83] G. G. Emch, J. Math. Phys. **7**, 1198 (1966).

[84] C. Radin, J. Math. Phys. **11**, 2945 (1970).

[85] M. Kastner, Phys. Rev. Lett. **106**, 130601 (2011).

[86] B. Vermersch, A. W. Glaetzle, and P. Zoller, Phys. Rev. A **91**, 023411 (2015).

[87] A. Derevianko, P. Kómár, T. Topcu, R. M. Kroeze, and M. D. Lukin, Phys. Rev. A **92**, 063419 (2015).

[88] E. A. Goldschmidt, T. Boulier, R. C. Brown, S. B. Koller, J. T. Young, A. V. Gorshkov, S. L. Rolston, and J. V. Porto, Phys. Rev. Lett. **116**, 113001 (2016).

[89] C. Gaul, B. J. DeSalvo, J. A. Aman, F. B. Dunning, T. C. Killian, and T. Pohl, Phys. Rev. Lett. **116**, 243001 (2016).

[90] B. J. DeSalvo, J. A. Aman, C. Gaul, T. Pohl, S. Yoshida, J. Burgdorfer, K. R. A. Hazzard, F. B. Dunning, and T. C. Killian, Phys. Rev. A **93**, 022709 (2016).

[91] S. Ye, X. Zhang, T. C. Killian, F. B. Dunning, M. Hiller, S. Yoshida, S. Nagele, and J. Burgdorfer, Phys. Rev. A **88**, 043430 (2013).

[92] A. Schwarzkopf, D. A. Anderson, N. Thaicharoen, and G. Raithel, Phys. Rev. A **88**, 061406(R) (2013).

[93] P. McQuillen, X. Zhang, T. Strickler, F. B. Dunning, and T. C. Killian, Phys. Rev. A **87**, 013407 (2013).

[94] G. Günter *et al.*, Science **342**, 954 (2013).

[95] N. Takei *et al.*, Nat. Commun. **7**, 13449 (2016).

[96] A. Reinhard, T. C. Liebisch, B. Knuffman, and G. Raithel, Phys. Rev. A **75**, 032712 (2007).

[97] T. G. Walker and M. Saffman, Phys. Rev. A **77**, 032723 (2008).

[98] I. I. Ryabtsev, D. B. Tretyakov, I. I. Beterov, V. M. Entin, and E. A. Yakshina, Phys. Rev. A **82**, 053409 (2010).

[99] J. Zeiher *et al.*, Nat. Phys. (to be published online 2016).

[100] J. Schachenmayer, A. Pikovski, and A. M. Rey, New J. Phys. **17**, 065009 (2015).

[101] J. Schachenmayer, A. Pikovski, and A. M. Rey, Phys. Rev. X **5**, 011022 (2015).

[102] J. Schachenmayer, L. Pollet, M. Troyer, and A. J. Daley, Phys. Rev. A **89**, 011601 (2014).

[103] L. Pucci, A. Roy, and M. Kastner, Phys. Rev. B **93**, 174302 (2016).